6th Congress of Alps-Adria
Acoustics Assosiation
16.-17. October 2014
Graz, Austria

Austrian Acoustics Association
Österreichische Gesellschaft für Akustik

Alps Adria Acoustics Association

ISBN: 978-3-200-03921-6

TEST SIGNAL FOR IDENTIFICATION OF NONLINEAR RESPONSE IN ELECTROMECHANICAL SYSTEM

Jurij Prezelj, Mirko Čudina

Prezelj.jurij@gmail.com, *Faculty of mechanical engineering, University of Ljubljana*

Abstract: *Fullrange loudspeakers are used in this article as an example of electromechanical system with nonlinear behaviour. Fullrange loudspeakers tend to have diameters smaller than 6″. Due to their small size they have to work with long cone excursions to achieve sufficient sound pressure levels in lower frequency range; therefore they are prone to the nonlinear distortion. Different methods were already developed for identification of different types of nonlinear distortions produced by electromechanical system. All these methods use well known test signals together with extensive digital signal processing, especially transformations from time domain into frequency domain and vice versa. Only few researchers observed nonlinear distortions in the original time domain; however they used only well-established test signals. A different test signal is proposed in this article. New test signal enables very fast and lucid identification of cumulative nonlinear distortions. By using this proposed test procedure, the nonlinear effect can be easily quantified for the purpose of comparing and evaluating different electromechanical systems. A new approach of incorporating a simple nonlinear operator into the convolution integral, for the purpose of simulating the nonlinear responses, is introduced in this article as well. Results of measurements, using proposed signal, and simulations, using convolution with incorporated nonlinear operator, are in good agreement and validate each other.*

Key words: nonlinearity, test signal, electromechanical system, nonlinear operator, fullrange loudspeaker

1. INTRODUCTION

Electromechanical systems, in a real environment are generally time invariant and include nonlinearity. Hence, a single linear model does not precisely match these systems. Nonlinearity is usually determined from additional measured responses of the system at different levels of input signal, [1, 2].

Impulse response measurements of electro-mechanical systems are frequently performed for system characterization and modeling. These measurements are affected with noise and with nonlinearity of the measured system, among others. While measurement noise may be reduced by increasing the length of the excitation signal and by averaging the outputs from several excitations, nonlinearity is an inherent problem for such techniques and is difficult to be characterized accurately.

Identification of relatively simple nonlinear systems is possible using iterative procedures, although this is complicated by the requirement for reasonably accurate initialization, [3]. Kemp and Primack compared two such methods for nonlinear system identification; Diagonal Volterra model and Exponential sine sweep [4]. Both processes are time consuming and demands automatize measurement equipment and data analysis. There are also numerous other methods for identification of nonlinear effects within the electromechanical system, however they all demand sophisticated equipment and extensive signal processing. In order to simplify the process of evaluating the effects of nonlinearity in electromechanical systems, a new method for numerical modeling of nonlinearity was developed.

Small fullrange loudspeakers were selected as test object because they are rarely studied in literature, despite the wide range of embedded products using this type of loudspeaker. Additionally, developing a better loudspeaker should be a relevant solution to improve the global quality of the system. Despite the technological process improving, a low-cost loudspeakers used in multimedia devices are still highly non-linear, [5].

In a conventional loudspeaker system, the source of nonlinearity is mainly the loudspeaker unit. The loudspeaker nonlinearities depend on displacement of the coil x (Fig.1) and on the electrical current in the voice coil, [5]. x_{lin} depicts the limit within the loudspeaker works as linear system. x_{max} depicts the maximum displacement within the loudspeaker is working, and x_{damage} is the limit after which the loudspeaker is damaged. Sources of nonlinearity are directly related to the geometry and material properties of the internal components, [2]. Nonlinearities, which produce distortions, can be classified into three categories. The first type corresponds to the motor nonlinearities, second type corresponds to the suspension nonlinearities, and the third type corresponds to the acoustical nonlinearities. The last source of nonlinearity is not described here since these nonlinearities are directly produced only if sound pressure level exceeds 130 dB. This is not possible with small fullrange loudspeaker, [6].

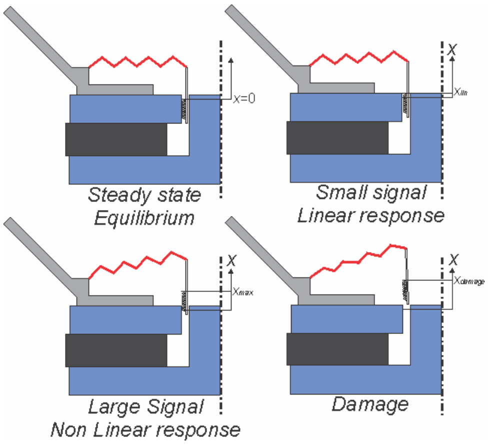

Fig. 1: Working range of loudspeaker

1.1. The motor structure

Dependence of the force factor $B_r l$ on the displacement $x(t)$ of the coil is among the major sources of nonlinearities [2]. It can be observed by comparing the level ratio of different harmonics. The odd harmonics are much more affected by this source of nonlinearity than the even harmonics [5]. The force factor Bl is not uniform across the air gap. Therefore, the force factor depends on the voice coil position. Indeed, the magnetic field induction B is the superposition of two fields. One of them is created by the permanent magnet and is time independent. This field crosses through the yoke pieces but only 30 % serves to move the coil, [6]. The other one is created by the coil and is time dependent. Klippel proposed to model the force factor by using a 2nd order polynomial, [2];

$$Bl(x)=Bl_0+Bl_1x+Bl_2x^2 \qquad (1)$$

In reality, the force factor depends on the displacement x of the voice coil, and this variation is not symmetrical relative to the equilibrium position. Its model of dependence can be found by using a 4th order polynomial function, [7].

1.2. The voice coil inductance

The coil self-inductance depends on the moving part position. This dependence generates a reluctant force. This reluctant force is given by, [6]:

$$Frel(t) = \frac{1}{2} i(t)^2 \frac{dLe(x)}{dx} \qquad (2)$$

We see that when the inductance L_e does not depend on the voice coil position x, the reluctant force $F_{rel}(t)$ equals zero. This is actually one of the assumptions of the Small signal model using lumped parameters.

1.3. Eddy currents

The electrical conductivity of the iron is high enough to let the eddy currents appear in the iron yoke pieces of the motor. Vanderkooy proposed a model which takes this phenomenon into account. The interaction between the eddy currents and the current in the coil generates a drag force F_{drag} which can be written as follows, [8]:

$$F_{drag} = \mu(i,x) \frac{dx(t)^{1,7}}{dt} \qquad (3)$$

Where μ (i,x) can be defined as the sensitivity of the drag force, according to the eddy currents. Force therefore depends on the input current, and on the position of the voice coil within the magnetic field.

1.4. The suspension

A classical suspension is mostly made of rubber, impregnated fabric or molded plastic. The small signal model using lumped parameters describes a suspension as an ideal spring, but an actual suspension always shows nonlinear behavior. In consequence, its compliance C_{ms} depends on the movement amplitude and the induced damping parameter depends greatly on both; the amplitude and frequency. More generally, many authors use the mechanical stiffness k which is defined by:

$$k=1/C_{ms} \qquad (4)$$

Like the force factor Bl, k can be written in terms of the 2nd order polynomial function.

$$k(x)=k_0+k_1x+k_2x^2 \qquad (5)$$

Such a model has been used by Klippel [2], to model the nonlinear behavior of both; the outer rim, and the spider. However, such model cannot take into account the effect of the hysteretic response of elastomers.

2. MODELING THE NONLINEARITY

Sources of nonlinearity in the loudspeaker usually reduce its response at higher amplitudes. Level of such reduction depends on the loudspeaker construction and on the amplitude of the driving signal. There are more available numerical models for describing the nonlinearity of the electromechanical systems. Two most common are the Volterra series and the Hammerstein model.

2.1 Volterra series

A Volterra series characterizes a causal and time-invariant nonlinear system with a straightforward filter structure, in which the system (input–output equation) is rendered as a polynomial series. Due to the advantage that Volterra series expansion is a linear combination of nonlinear functions of the input signal, adaptive Volterra filters are well suited for modeling of nonlinear systems and for using the nonlinear system identification algorithms, such as the least-mean-square (LMS) algorithm and the recursive least-square (RLS) algorithm.

Assume $x(n)$ and $y(n)$ represent the input and output signals, respectively. The polynomial series based Volterra series is given by the following expression, [9].

$$y(n) = h_0 + \sum_{m1}^{\infty} h_1(m_1)x(n-m_1) + \sum_{m_1=0}^{\infty}\sum_{m_2=0}^{\infty} h_2(m_1 m_2)x(n-m_1)x(n-m_2) + \cdots + \sum_{m_1=0}^{\infty}\sum_{m_2=0}^{\infty} \ldots \sum_{m_p=0}^{\infty} h_p(m_1, m_2, \ldots m_p)x(n-m_1)\,x(n-m_2)\ldots x(n-m_p) \quad (6)$$

Where $h_p(m_1, m_2, \ldots, m_p)$ is defined as the p-th order Volterra kernel, and h_0 is a constant value, which can be ignored in the adaptive filtering. Actually, h_p can be regarded as impulse response for different types / rates of nonlinearities. Matrix $h_p(m_1, m_2, \ldots, m_p)$ is assumed to be symmetric.

Simulation and measurement results in [13] show that the Volterra series is very suitable to characterize the nonlinear behavior of the electromechanical system. The quadratic nonlinearity is largely dominated by the first coefficient of the 2nd order kernel. Experimental comparison showed that the Volterra model can effectively and accurately predict the sound pressures and harmonic distortions within the bandwidth of the training signal, [9].

Volterra models can be seen as a generalization of the simple convolution operator used for linear systems. Such models represent exactly any nonlinear analytical system, and approximate any nonlinear system with a fading memory. Measurement methods were already developed to identify the first two or three terms of the Volterra series. These experimental methods are time consuming because they require many measurements. Moreover the difficult physical interpretation of the different terms of the Volterra series limits its use, [10].

2.2 Hammerstein model

While the completely general modeling of a nonlinear system requires a convolution, which involves a multidimensional matrix with the same number of dimensions as the order of the distortion, as shown in the Volterra series (Eq.6), a useful simplified model may be obtained by using only the diagonal elements of this multidimensional matrix. This method was set out by Reed, [13], and it can be expressed in time domain as given in [11, 12]:

$$y(n) = h_0 + \sum_{m1}^{\infty} h_1(m_1)x(n-m_1) + \sum_{m1}^{\infty} h_2(m_1)x^2(n-m_1) + \sum_{m1}^{\infty} h_3(m_1)x^3(n-m_1) + \cdots \quad (7)$$

Where h_m is the response of the system to the p-th power of the input. For obtaining responses $h_i(m)$, involves taking the powers of the input signal in the time domain and then using the Fourier transform to compute convolutions. This method presupposes that the input signal is periodic, and this condition may be achieved during measurements by playing the input signal twice and analyzing the signal obtained during the second play.

In this method, each impulse response $h_p(m)$ is convolved with the input signal $x(n)$ elevated to its p-th power and the output $y(n)$ is the sum of these convolutions. The first impulse response $h_1(n)$ represents the linear response of the system. The other impulse responses h_1, h_3 … h_P model the nonlinearities, [3,10].

The family of impulse responses is usually referred to as the Kernel of the model. This Kernels is assumed to be integrable. Any cascade of Hammerstein models is fully represented by its Kernels. It can easily be shown that cascade of Hammerstein models correspond to Volterra models having diagonal Kernels in the temporal domain. This nonlinear model is thus referred in the literature as a diagonal l Volterra model, but also as a cascade of Hammerstein models, or Uryson model, [10].

2.3 Proposed simplified model with a numerical operator for the nonlinearity

Dominant sources of loudspeaker nonlinearity loudspeaker reduce its response at higher amplitudes. Level of the response reduction depends on the construction of the loudspeaker driver and on the amplitude of driving signal. Sources of nonlinearities are generally described with polynomial; however, much more straightforward approach by using simple trigonometric function can also be used. Influence of nonlinear magnetic flux, with weak smooth nonlinear characteristics, can be described with Eq.8, [14], as depicted in Fig. 2 for different rates of nonlinearity.

$$\mathrm{N}\{s(t)\} = \frac{\arctan\left(k_{nonlin} s(t)\right)}{k_{nonlin}} \quad (8)$$

If Eq.8 is to be applied as an operator N(s), then a question appears; where to apply it? On the input signal $x(t)$, on the output signal $y(t)$, or within the convolution integral itself, as indicated with the Hammerstein model? Equations with different position of the nonlinear operator $N\{s(t)\}$ are given in the Table 1.

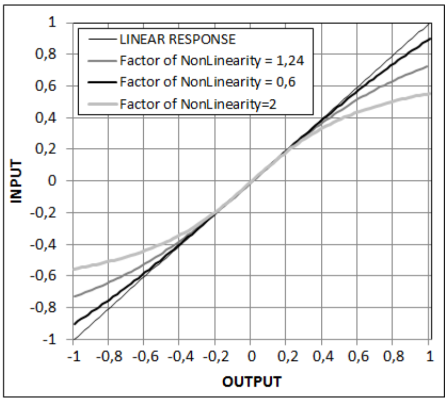

Fig. 2: Nonlinear operator for simplified nonlinear system at different rates of nonlinearity k_{nonlin}

Table 1: Application of nonlinear operator N

operator N at:	Equation
INPUT	$y_N(t) = h(n) * \mathrm{N}\{x(t)\}$
OUTPUT	$y_N(t) = \mathrm{N}\{y(t)\} = \mathrm{N}\{h(n) * x(t)\}$
CONVOLUTION	$y_N(t) = \sum_{n=1}^{T_0} [\mathrm{N}\{h(n) * x(t-n)\}]$

Each position of the nonlinear operator $N\{s(t)\}$ provides a different result, as depicted with the set of resulting numerical equations given in Table 2. In order to establish how to properly use nonlinear operator $N\{s(t)\}$, a set of simulations was performed using numerical solutions given in Table 2 and using white noise and impulse response. Results are presented in chapter 5.

Table 2: Numerical calculations for modeling

operator N at:	Numerical
INPUT	$y(t) = \sum_{n=1}^{N} h_0(n) \frac{\mathrm{k_{nonlin}} \arctan(x(t-n))}{k_{nonlin}}$
OUTPUT	$y(t) = \frac{arctan(k_{nonlin} * \sum_n^N x(t-n) h_0(n))}{k_{nonlin}}$
CONVOLUTION	$y(t) = \sum_{n=1}^{N} \frac{arctan(k_{nelin}\, x(t-n) h_0(n))}{k_{nelin}}$

In order to be able to compare simulation results in time domain, with measured impulse responses, a new test signal was developed. The main purpose of the new test signal was to speed up the process of measurements and to enable the visual perception of the nonlinearity effect directly in the time domain. Test signal was also designed for the purpose to obtain kernel of impulse responses for different rates of nonlinearity with a single measurement sequence.

2.5. Proposed test signal

Proposed test signal is depicted in Fig.3. Test signal is combined from two functions; from the harmonic function representing the carrier signal with subsonic frequency and from the Kronecker delta function, which is usually defined on a finite domain. Kronecker delta function takes values 0 and 1 and is theoretically broadband in frequency domain. Its representation in frequency domain is theoretically similar to random signal / white noise. Frequency of the harmonic function was set to 7 Hz and is well below audible range and working range of any fullrange loudspeaker. This part of the signal is used to harmonically move the loudspeaker motor from the linear into the nonlinear working range. Impulses are used for the basic identification of system response. While the amplitude of the subsonic signal linearly decreases, the amplitude of the impulses remains the same relative to the baseline of the carrier signal, as depicted in Fig.3.

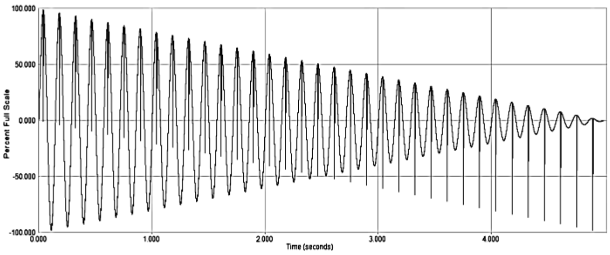

Fig. 3: Proposed test signal

If the loudspeaker is excited with a proposed signal with low amplitude, the loudspeaker can be considered as a linear system, even if it is not entirely true due to the dependence on electric current. As presented in Fig. 1, the nonlinearity needs to be taken into account only for excitation signals with higher amplitudes, when the loudspeaker coil starts to perform large strokes. It is therefore necessary to take into account the rate of displacement over time to correctly model the loudspeaker nonlinearity, [5]. Proposed signal does exactly that. It enables fast and simple measurements of the nonlinearity effect at different levels of the crucial part of the input signal which causes the nonlinear response.

3. MEASUREMENT SETUP

Measurements were performed in the anechoic chamber, (Fig.4) with volume of 36 m^3. Signal from the measurement microphone B&K type 4940 was amplified with the measurement amplifier B&K type 2636 and sampled with A/D converter set to 192 kHz sampling rate and 24 bit resolution. Power amplifier for driving the loudspeakers was based on TDS7294, and provided 100 W(rms) power. Acoustic measurements were performed with a microphone and loudspeakers at a fixed position. Proposed test signal was reproduced two times at each amplification level. Amplification level was gradually increased from -42 dB to -18 dB.

Proposed test signal was used for evaluation of two fullrange loudspeaker with effective piston area of 31 cm^2 and 38,5 cm^2. Two signals were measured; sound pressure signal and electric current. Electric current was measured via voltage drop on 2 Ohm resistor connected in line. During the measurements, the amplification was set to deliver equal RMS value of electric current on both tested loudspeakers.

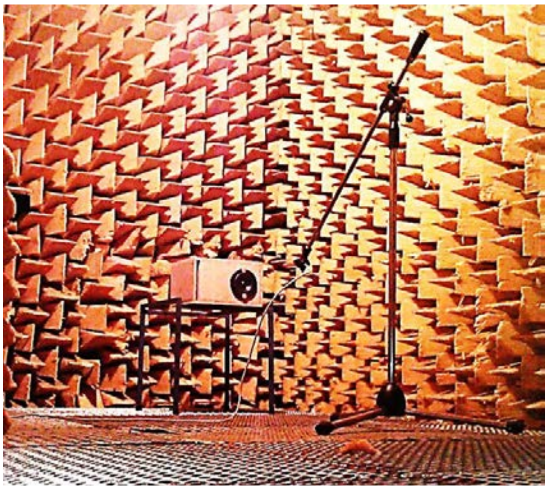

Fig. 4: Measurement setup

4. MEASUREMENTS RESULTS

Fullrange loudspeaker cannot produce sound pressure at the subsonic frequency of the carrier signal at 7 Hz as it can be seen from measurement results presented in Figs. from 5 to 7. Such a low frequency cannot be reproduced due to small dimensions and too low excursion of loudspeaker membrane. Although the membrane was actually moving accordingly with the signal during the experiment no sound with such a low frequency was generated. In our experiment a Fullrange loudspeakers was therefore actually working as a high pass filters. While loudspeakers were able to reproduce impulses they completely filtered out the subsonic component of the test signal. However, this subsonic component of the test signal has significant influence on the performance of the loudspeaker.

In the first experiment the proposed test signal was tested by observing the response of a loudspeaker FRS8. Response of the loudspeaker was observed at five different levels of the proposed test signal. Results are depicted in Fig. 5, where 2 sequences of the test signal are recorded for five amplification levels;
(-42 dB, -36 dB, -30 dB, -24 dB and -18 dB).

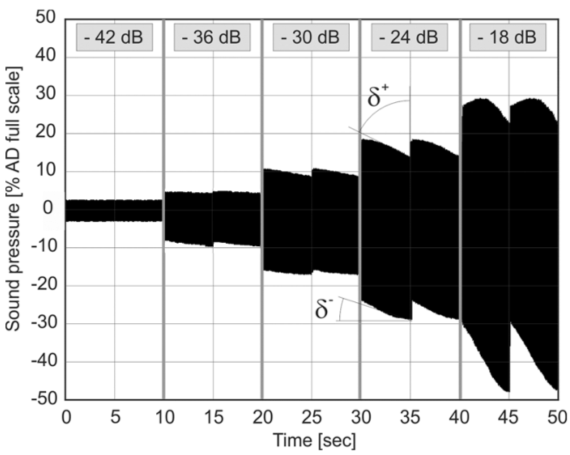

Fig. 5: Response of the fullrange loudspeaker FRS8 to the test signal

If the amplitude of the test signal is low (Fig.5, -42 dB), then the loudspeaker easily generates impulses within the test signal, regardless to the amplitude of the subsonic part of the test signal and amplitudes of the generated impulses remain constant. Influence of the subsonic part of the signal on the impulse response of the loudspeaker can be observed only at higher amplification levels, as expected. If the amplitude of the test signal is higher (Fig.5, -18 dB) then the loudspeaker cannot generate impulses within the test signal with ease, and the amplitudes of the generated impulses depend on the amplitude of the subsonic part of the test signal.

At the start of the test signal, the energy of the subsonic part dominates within the RMS value. At the end of the signal only impulses remain within the test signal and RMS value of the signal depends only on the amplitude of impulses. If the loudspeaker is excited with low levels of the proposed signal, then the subsonic part of the signal does not push the loudspeaker motor outside the linear part of the driver motor. At increased level of the signal, the subsonic part of the signal pushes the coil outside the linear part of the driver motor and superimposed impulse response is adequately altered, according to the effect of nonlinearity. When the amplitude of the subsonic part of the signal is decreased, the coil is working within the linear part of the driver motor, and the impulse response adequately returns to the linear response.

Measurement results of 8 reproductions of proposed test signal with FRS8 loudspeaker are depicted in Fig.6. Measurement results of 10 reproductions of the proposed test signal with B80 loudspeaker are depicted in Fig.7. Overall RMS value of the electric current signal was kept constant for both tested loudspeaker, resulting a in a test signal level at -24 dB for the loudspeaker B80 and -29 dB for the loudspeaker FRS8.

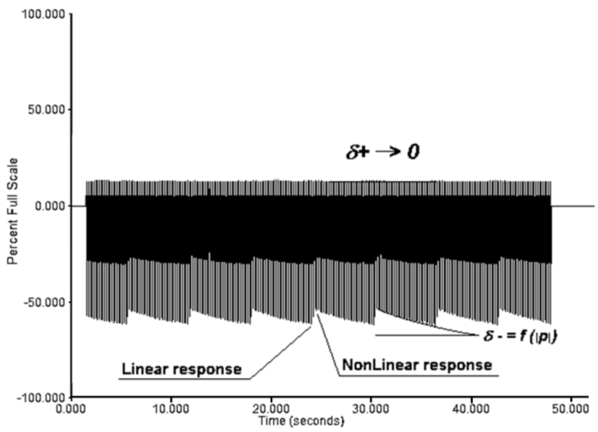

Fig. 6: Response of the fullrange loudspeaker FRS8 to the test signal presented in Fig.3, at -36 dB

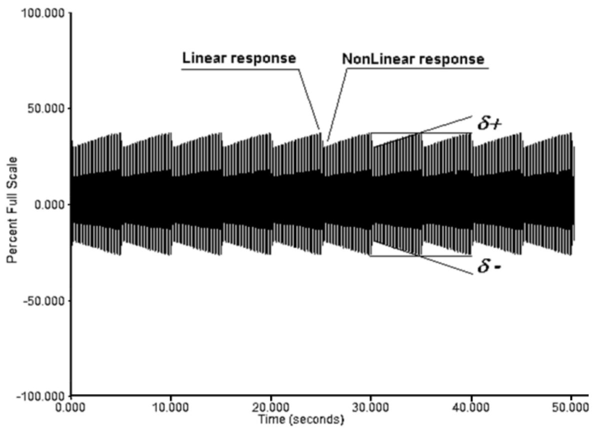

Fig. 7: Response of the fullrange loudspeaker B80 to the test signal presented in Fig.3, at -31 dB

Envelope of the measured sound pressure peaks can be used as an indicator/estimator for the rate of nonlinearity. Impulse amplitude change rate δ can present a deviation function of nonlinear response relative to linear one. Index + indicate positive part of the impulse response and index - indicates its overshoot. If the loudspeaker is working in linear range, then both; δ+ and δ - are limited toward 0. If the loudspeaker works outside the linear range both function significantly increase.

A Comparison between the impulse responses of the fullrange loudspeaker when working in linear range and in nonlinear range are presented in Fig.8 and Fig.9, for two different fullrange loudspeakers (FRS8 and B80). In both figures, the linear impulse response is presented with thin black line and impulse response with nonlinear behavior is depicted with thick grey line.

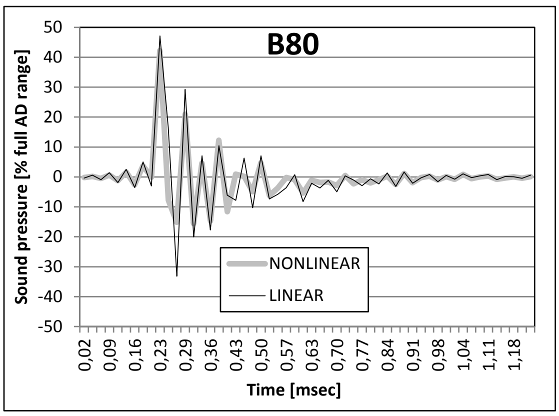

Fig.8. Comparison between two different measured impulse responses of fullrange loudspeaker B80; linear – thin black curve and nonlinear – thick grey curve

In both cases we can see that high amplitude of subsonic part of the signal (Nonlinear part) reduces the amplitude of the impulse response. We can observe effect of nonlinearity in impulse response of the loudspeaker B70 from the first peak up to the eighth peak. On the other hand, nonlinear distortion affects only the amplitude of the firs peak in the impulse response of the fullrange loudspeaker FRS. Nonlinear impulse response of FRS8 is obviously less affected by subsonic signal component as nonlinear impulse response of B80.

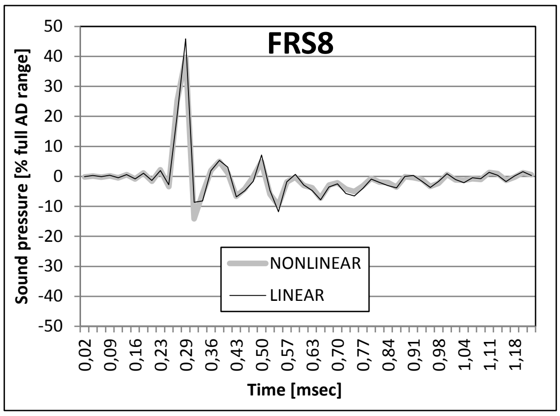

Fig.9. Comparison between two different measured impulse responses of fullrange loudspeaker FRS8; linear – thin black curve and nonlinear – thick grey curve

Proposed new test signal enables lucid observations of loudspeaker deviation from linearity already in time domain. Consequently, a quantification of nonlinearity can be easily performed directly from the measured sound pressure signals. Two measured impulse responses were also used later to calculate the transfer function in frequency domain and compared with simulation results.

5. SIMULATIONS

Sources of nonlinearities are usually described with polynomials; however, during the observation of measurement results and results from a theory, a more simplified approach immerged by using a simple trigonometric function, as depicted in Fig.2 and given by Eq. 8 Such approach is primarily intended for modeling the time invariant systems of the first order. Its applicability for modeling the nonlinearities in the loudspeaker could not be found in the literature. Therefore a set of simulations was conducted according to Table 2 to establish the usability of nonlinear operator. The purpose of the simulations was to find the proper way to incorporate the nonlinear operator into the numerical calculations of the nonlinear convolution.

Three different position of nonlinear operator were taken into account;

- nonlinear operator on the input signal, $\mathrm{N}\{x(t)\}$,
- nonlinear operator on the output signal, $\mathrm{N}\{y(t)\}$,
- nonlinear operator within the convolution,

$$\sum_{n=1}^{T_0}\left[\mathrm{N}\{h(n)*x(t-n)\}\right] \tag{9}$$

for two different test signals;

- Kronecker delta function and
- white noise.

Results of simulations are depicted in Figs. 10 and 11. Influence of the nonlinear operator position on the impulse response is depicted in Fig. 10. Black thin curve depicts the linear impulse response of the loudspeaker, grey thin curve depicts the nonlinear impulse response simulated by the nonlinear operator applied on the input signal $x(t)$. Grey thick curve depicts the nonlinear impulse response simulated by nonlinear operator applied on the output signal y(t). Nonlinear impulse response of the system, calculated with the nonlinear operator incorporated into the convolution, is identical to the nonlinear impulse response simulated by nonlinear operator applied on the output signal. In case of the excitation of the nonlinear system with the impulse, a following equation can be written;

$$y_N(t) = \mathrm{N}\{y(t)\} = \mathrm{N}\{h(n) * x(t)\} = \sum_{n=1}^{T_0} \left[\mathrm{N}\{h(n) * x(t-n)\}\right] \qquad (10)$$

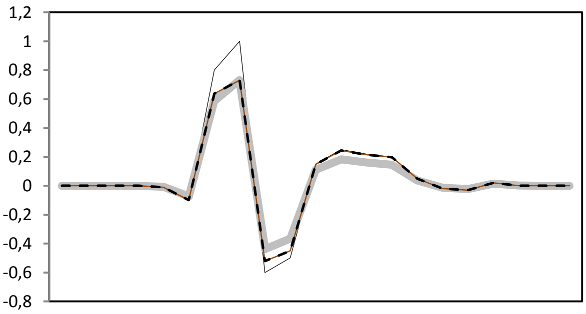

Fig.10. Simulation results of loudspeaker impulse response for three different location of the nonlinear operator.

Influence of the nonlinear operator position on the simulated white noise response is depicted in Fig. 11. Thin black curve depicts the signal of linear system response to white noise, grey curve depicts the nonlinear system response to white noise, simulated by the nonlinear operator applied on the input signal $x(t)$. Grey thick curve depicts the nonlinear impulse response simulated by nonlinear operator applied on the output signal y(t). Black dotted line represents the simulated signal response for the nonlinear operator within the convolution.

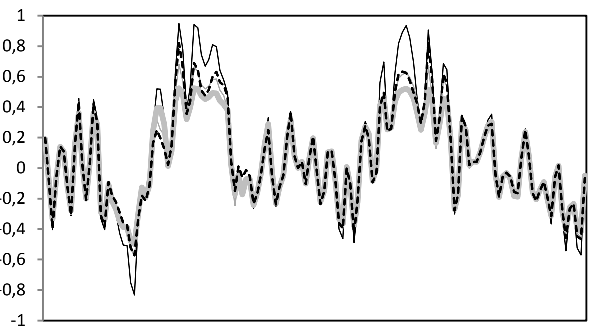

Fig.11. Simulation results of loudspeaker response to white noise using three different positions of the nonlinear operator.

Two measured impulse responses were used to calculate the transfer function in frequency domain. Results of simulations were later also used to determine the frequency response of the linear and nonlinear loudspeaker. Analysis of simulation results, especially the frequency analysis of simulated signals, showed that the most appropriate placing of the simple nonlinear operator is within the convolution integral (convolution series). Comparison between the simulation results and measurement results are depicted in Fig.12 for loudspeaker FRS8 and in Fig.13 for the loudspeaker B80. Linear frequency response is depicted with thin black line and nonlinear response is depicted with thick grey line. Comparison between simulations and measurement results indicate that simple nonlinear operator can be implemented within the convolution sum to obtain good results in modeling the nonlinearity. Additional advantage of proposed procedure is that a single value can be used for describing the effect of nonlinearity of the loudspeaker.

The main purpose of presenting the results in frequency domain is to show that characteristic of fullrange loudspeaker alters significantly if the loudspeaker is working in the linear or in the nonlinear range. Frequency domain is generally used for description of loudspeaker performance, even though description in frequency domain is only a transformation from the time domain.

From all presented results we can conclude that the proposed test signal enables lucid observations of loudspeaker deviation from linearity already in time domain. Consequently, a quantification of nonlinearity can be easily performed directly from the measured sound pressure signals.

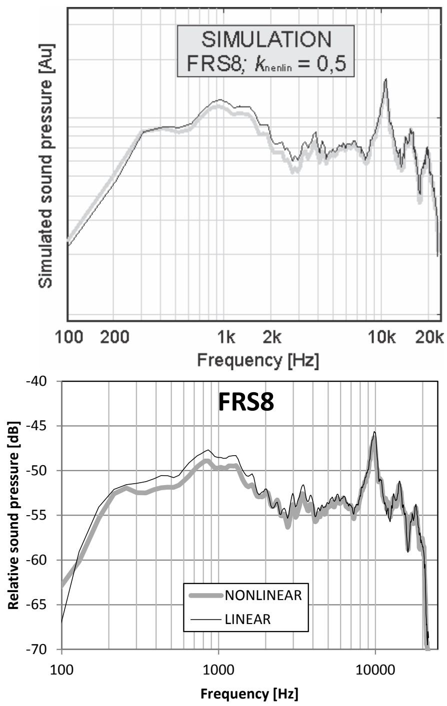

Fig.12. Simulated effect of nonlinearity (above) and measured effect of nonlinearity using proposed test signal (below) for loudspeaker FRS8

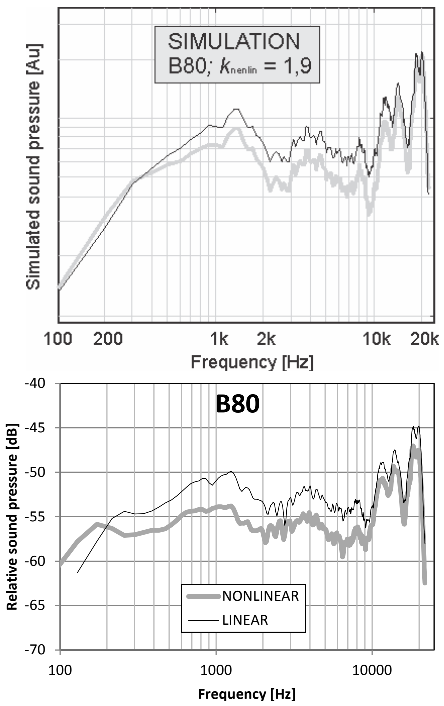

Fig.13. Simulated effect of nonlinearity (above) and measured effect of nonlinearity using proposed test signal (below) for loudspeaker B80

6. CONCLUSIONS

Nonlinear distortions can be easily observed in raw microphone signal if proposed test signal is used for the excitation of the loudspeaker. Quick and lucid comparison of loudspeaker drivers and their nonlinearity rate can be performed already in time domain without any need for additional signal processing.

Nonlinear impulse response, induced by subsonic component in the test signal, can be modeled by simple nonlinear operator given in Eq.9. Analysis of simulation results, especially the frequency analysis of simulated signals, showed that the most appropriate position of the simple nonlinear operator is to be within the convolution integral, (convolution series). Measurement results and simulations with such nonlinear convolution are in good agreement, validating the applicability of the proposed test procedure and proposed modeling of the nonlinearity at the same time.

7. REFERENCES

[1] Shoichiro Saito, Akira Nakagawa, and Yoichi Haneda, Dynamic impulse response model for nonlinear acoustic system and its application to acoustic echo canceller, 2009 IEEE Workshop on Applications of Signal Processing to Audio and Acoustics October 18-21, 2009, New Paltz, NY

[2] W. Klippel, Tutorial "Loudspeaker Nonlinearities- Causes, Parameters, Sysmptoms", J. Audio Eng. Soc. Vol. 54, Number 10, pp. 901-939 (2006 Oct.).

[3] Philips Crama and Johan Schoukens, Wiener Hammerstein System Estimator initialisation using a Random MultiSine excitation, ARFTG, Conference Digest Full, Vol.40, pp.1-6, 2001.;

[4] Jonathan Kemp, Harel Primack, Impulse response measurements of Nonlinear systems: Properties of existing techniques and wide noise sequences, J.Audio Eng. Soc., Vol. 59, No. 12, pp. 953-963, 2011 December

[5] E. Sturtzer, G. Pillonnet a, G. Lemarquand b, N. Abouchi a, Comparison between voltage and current driving methods of a micro-speaker, Applied Acoustics 73 (2012) 1087–1098

[6] R. Ravaud, G. Lemarquand, T. Roussel, Time-varying non linear modeling of electrodynamic loudspeakers, Applied Acoustics 70 (2009) 450–458

[7] B. Merit, G. Lemarquand *, V. Lemarquand, Performances and design of ironless loudspeaker motor structures, Applied Acoustics 71 (2010) 546–555

[8] J. Vanderkooy, W.R. Datars, Nonlinear effects in the de Haas-van Alphen effect, Physics Letters A, Volume 25, Issue 3, 14 August 1967, Pages 258–259

[9] Wei Ji, Woon Seng Gan, Identification of a parametric loudspeaker system using an adaptive Volterra filter, Applied Acoustics 73 (2012) 1251–1262

[10] Marc Rebillat, Romain Hennequin, Etienne Corteel, Brian F.G.Katz, Identification of cascade of Hammerstein models for the description of nonlinearities in vibrating devices, Journal of Sound and Vibration, 330, (2011), pp.1018–1038

[11] Angelo Farina, Simultaneous Measurement of Impulse Response and Distortion with a Swept-Sine Technique, presented at the 108th Convention of the Audio Engineering Society, Convention paper 5093, February 2003;

[12] Angelo Farina, Advancements in Impulse Response Measurement Sine-Sweeps, presented at the 122nd Convention of the Audio Engineering Society, Convention paper 7121, May 2007;

[13] M. J. Reed, M.O.Hawksford, Practical systems modelling using of nonlinear the Volterra audio series, AES 100th convention, 1996, May 11-14, Copenhagen

[14] L. Půst, Nonlinear effects on the rotor driven by a motor with limited power, Applied and Computational Mechanics 1 (2007), pp. 603 – 612